J Appl Electrochem (2010) 40:1875–1881
DOI 10.1007/s10800-010-0150-6

ORIGINAL PAPER

Synthesis and characterization of $La_{0.75}Sr_{0.25}Cr_{0.9}M_{0.1}O_3$ perovskites as anodes for CO-fuelled solid oxide fuel cells

K. M. Papazisi · S. Balomenou · D. Tsiplakides

Received: 11 February 2010 / Accepted: 17 May 2010 / Published online: 3 June 2010

Abstract A series of $La_{0.75}Sr_{0.25}Cr_{0.9}M_{0.1}O_3$ (M = Mn, Fe, Co, Ni) perovskite compounds was synthesized by a modified citrate sol-gel route and employed as anode electrodes on YSZ electrolyte supported SOFC cells. Materials and anode electrodes were characterized for their chemical composition, crystal structure and film morphology. The electrochemical performance of the prepared anodes was evaluated in button cells under SOFC operation with CO/CO_2 mixtures in the temperature range of 900–1000 °C. It was shown that the performance of the perovskite materials in terms of maximum power density follows the sequence Fe > Ni > Co > Mn, based on the substitution cation into the B-site. No carbon deposition was observed under the operating conditions examined, even for prolonged (120 h) exposure to the reaction mixture.

Keywords Solid oxide fuel cell · Anode materials · Perovskite · $La_{0.75}Sr_{0.25}Cr_{0.9}M_{0.1}O_3$ · CO · Carbon deposition

K. M. Papazisi · S. Balomenou · D. Tsiplakides (✉)
CPERI/CERTH, 6th km Charilaou-Thermi Rd,
57001 Thessaloniki, Greece
e-mail: dtsiplak@chem.auth.gr

K. M. Papazisi
Department of Chemical Engineering, Aristotle University of Thessaloniki, 54124 Thessaloniki, Greece

D. Tsiplakides
Department of Chemistry, Aristotle University of Thessaloniki, 54124 Thessaloniki, Greece

1 Introduction

Fuel cells represent probably the most promising technology for clean energy production and a gasoline free source of propulsion. Additionally to low or zero emissions, fuel cells offer many advantages such as high efficiency and reliability, multi-fuel capability, low-cost easy maintenance and distributed power generation. Among the available fuel cell technologies, SOFCs appear to offer the greatest potential for stationary applications or combined heat and power generation (CHP) systems. Probably the most compelling factor driving the R&D efforts being directed at SOFC power systems is that, besides hydrogen, they can be directly fuelled by a wide range of conventional fuels such as natural gas, a convenient and readily available fuel in many countries in the world, hydrocarbon fuels, coal or biofuels [1]. Hydrocarbon or reformate fueled SOFCs face one major limitation related to carbon deposition at the anode electrode, suggesting a substantially short useful lifetime given the current technology. Most of the metals used as anode materials are very effective catalysts for hydrocarbon dissociation towards carbon formation, which takes place either via HC cracking (for example CH_4) or the Boudouard reaction:

$$CH_4 \rightarrow C_{gr} + 2H_2 \quad (1)$$

$$2CO \rightarrow C_{gr} + CO_2 \quad (2)$$

As a result anode degradation occurs, with high risk for overall cell failure. The formation of carbon depends on various parameters. The nature of the electrocatalyst plays a key role, for example, carbon deposition is favored on Ni (the most commonly used SOFC anode metal) rather than on Ru [2–4], Cu [5, 6] metals or perovskites [7–10]. The perovskite group of materials has attracted considerable

interest as an alternative for metals in SOFC electrodes. Research in this field goes back several years ago and there are comprehensive reviews of the studies conducted on the different ceramic anodes [11–13].

Due to their high electrocatalytic activity, high conductivity (ionic and electronic) in reducing atmosphere and sluggish carbon formation kinetics, these materials hold great hope for applications as a CO fueled SOFC. This technology is of high interest for space applications, specificaly related to Mars exploration, given that the Martian atmosphere is ~96% carbon dioxide. The CO_2 can be decomposed to CO and oxygen in order to supply the anode and cathode of a SOFC. There are very few attempts [14] to this direction and the reported work shows the possibility to develop a regenerative FC system for Mars based on an all-ceramic SOFC structure. Besides the above niche market, the CO-fueled SOFCs may also be utilized in terrestrial applications, for example in SOFCs fueled with biomass pyrolysis/gasification derived gases or in direct carbon fuel cells.

The understanding of the anode microstructure is substantial in order to identify and validate the perovskite material synthesis route which will enable control over the electrode behavior and allow the improvement of the cell performance.

2 Experimental

2.1 Powders preparation

A series of $La_{0.75}Sr_{0.25}Cr_{0.9}M_{0.1}O_3$ (M = Mn, Fe, Co, Ni) perovskite-type compounds, denoted LSC-M0.1 hereafter, was synthesized by the modified citrate/sol-gel route [15, 16]. After determining the metal content of the hygroscopic nitrates, the stoichiometric amounts of the corresponding metal nitrate, namely $La(NO_3)_3{\cdot}6H_2O$, $Sr(NO_3)_2$, $Cr(NO_3)_3{\cdot}9H_2O$ and $Mn(NO_3)_2{\cdot}4H_2O$, were dissolved in double distilled water and citric acid was added under heating (80 °C) and stirring. The mole ratio of citric acid:total metal ions was 2:1. Ammonia solution (25%) was introduced to obtain a pH value of around 9. With the evaporation of water, a dark coloured concentrated solution was obtained, which was further dried in an oven at 120–150 °C overnight. A black sponge-like material was obtained after heating at 200 °C for 2 h. The solid black foam obtained was finely ground and calcined under stagnant air, first at 500 °C for 5 h with a heating rate of 2 °C min^{-1} to decompose nitrates, cooled down to room temperature, and then at 1200 °C for 5 h with the same heating rate. The final temperature was chosen for ensuring thermal stability during electrocatalytic activity measurements within the range of 900–1000 °C.

2.2 Structural characterization

The crystal structure of the prepared materials was examined by X-ray diffraction. Powder XRD patterns were recorded with a Siemens D500 X-ray diffractometer, with auto divergent slit and graphite monochromator using Cu Kα ($\lambda = 1.5418$ Å) radiation, having a scanning speed of 2 min^{-1}. The characteristic reflection peaks (*d*-values) were matched with JCPDS data files and the crystalline phases were identified. The average crystallite size was calculated by means of the Scherrer formula after Warren's correction for instrumental broadening. The unit cell parameters were refined with the CrystalSleuth software.

The bulk concentrations of metal elements of the perovskite samples were determined by inductively coupled plasma-atomic emission spectroscopy (ICP/AES) analysis, carried out in a Plasma 400 (Perkin-Elmer) spectrometer, equipped with Cetac 6000AT+ ultrasonic nebulizer.

2.3 Button cells fabrication and characterization

A series of YSZ electrolyte-based button cells were prepared in order to evaluate the performance of the anode materials in SOFC operation. The YSZ pellets (Dynamic Ceramic, Technox 802) had a thickness of 1.6 ± 0.05 mm and a diameter of 20 mm. The anode and cathode electrodes had a geometric area of 1.55 cm^2. Commercially available LSM was used for the preparation of the cathode electrode in all samples (LSM20-I ink from NexTech Materials), while the synthesized perovskite powders were used for the preparation of the anode electrodes. Both LSCM (anode) and LSM (cathode) electrodes were deposited by air-pressurized spaying. The spray solution was a mixture of the LSM ink with terpineol ink vehicle (Fuel Cell Materials) with 30 wt% total solids and a mixture of the as-prepared powders with the ink vehicle with 20 wt% total solids for the cathode and anode, respectively. The resulting solution was pumped (syringe pump: Razel, motor 2 rpm) with a solution flow rate of 0.5 mL min^{-1} through a nozzle (Budger Air-brush Model 150), which was located 20 cm above the YSZ pellet and atomized by air pressure of 1 bar. The droplets were sprayed though a shadow mask onto the YSZ pellet with a spraying time of 140 s. These conditions resulted in a layer 21 ± 4 μm thick (LSC-Fe0.1 = 20 μm, LSC-Mn0.1 = 25 μm, LSC-Ni0.1 = 17 μm, LSC-Co0.1 = 20 μm) after appropriate calcination and sintering. The calcination and sintering profile which was followed was the same for the anode and cathode electrodes. It comprises of a first heating step with a rate of 3 °C min^{-1} up to 500 °C, dwell at this temperature for 2 h in order to decompose all the organic solvents, and a second heating step with the same

rate to 1100 °C (dwell for 2 h) in order to obtain uniform and continuous electrodes.

The morphology and structure of the prepared anode electrodes were examined by scanning electron microscopy (SEM) on a JEOL 6300 microscope, coupled with energy-dispersive X-ray analysis (EDX, Oxford Link ISIS-2000) for local elemental composition determination.

The electrochemical characterization and the performance evaluation of the button SOFC cells were carried out in a ProbostatTM measurement cell. The button cell was on top of an inner alumina support tube. By means of an outer closed alumina tube, the assembly forms two gas volumes separated by the cell. A 1 mm thick gold gasket was placed between the cell and the support tube. After heating to 1063 °C to soften the gold gasket, the detected leakage between inner and outer chambers was less than 200 ppm O_2. Electrode leads from the cell base were attached to the circular electrodes on the cell-from underneath (anode) inside the inner compartment, and on the top of the cell (cathode), from the outer gas compartment. Spring loads held the whole assembly together, to maintain good contact between the Pt leads and the electrodes at the surface of the cell and to facilitate good sealing. The inner and the outer compartment were fed with the CO/CO_2 mixture (0.9%/0.1% in He balance) and oxygen (1.36% in He balance), respectively, through mass flowmeters (Bronkhorst). This diluted atmosphere simulates the low atmospheric pressure conditions of Mars (1/100th of earth atmospheric pressure). A Princeton Applied Research potentiostat/galvanostat (Model 263A) was used for the electrochemical measurements.

3 Results and discussion

3.1 Physical, chemical and morphological characterization

The X-ray diffraction patterns of all synthesized materials, including a commercial LSM powder (Praxair) for comparison, are plotted in Fig. 1. They all reveal the presence of a single phase with rhombohedral distorted perovskite structure [17]. The lattice parameters are in the range of $a = 4.477$–5.498 Å, $c = 13.35$–13.47 Å and $V = 340$–352.7 Å^3, depending on the substitution cation into the B-site. The calculated lattice parameters are summarized in Table 1 together with those of the commercial LSM. It is expected that during exposure to reducing atmosphere (or equivalently when used as anodes in SOFCs) these materials exhibit phase transition to orthorhombic phase [18] accompanied by small changes in lattice parameters. Although the volume change during phase transformation is estimated to be about 1% for the bulk material, it causes

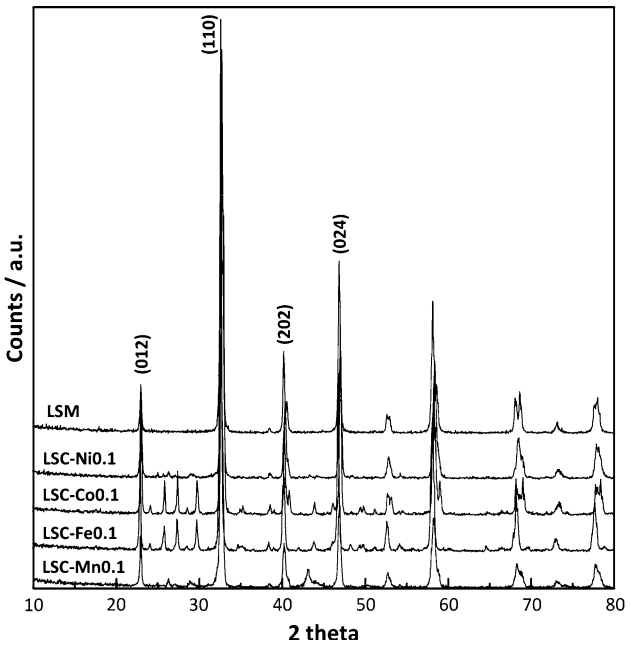

Fig. 1 X-ray diffraction patterns of the as synthesized $La_{0.75}Sr_{0.25}Cr_{0.9}M_{0.1}O_3$ powder samples and of a commercial LSM powder

significant changes in conductivity. On the other hand the small volume change explains the observed excellent bonding with the YSZ electrolyte under redox cycling throughout fuel cell preparation and testing, as concluded from the SEM pictures and the reproducibility of their fuel cell performance characteristics.

Some impurity phases, such as $SrCO_3$ or other metal carbonate phases can be identified at 25–30° (2θ) for some samples, as a result of metal carbonation in ambient atmosphere [19]. This is because these samples were calcined at lower temperature (900 °C), in order to facilitate their dissolution for carrying out the ICP analysis. It was, however, certified that these carbonate species are decomposed after calcination at 1200 °C.

The bulk concentrations of metal elements of the perovskite samples, as measured by ICP/AES, were found to be in good agreement with the nominal ones, with a maximum deviation from them lower than 5 at.%, which indicates the effectiveness of the materials preparation procedure.

Typical SEM micrographs showing the top view of the as-prepared LSCM electrodes are shown in Fig. 2a–d. Powders of the perovskite material were comprised of uniform particles with a homogeneous particle-size distribution in the submicrometric range. There are no significant differences in the microstructure among the electrodes, as it was also observed for the powder materials through XRDs calculations (Table 1). On average, these anodes show similar grain sizes, typically between 0.1 and 0.5 μm.

Table 1 Calculated unit cell parameters from XRD for different LSCM and LSM samples

Composition	α (Å)	c (Å)	Unit cell volume (Å^3)	Crystallite size (nm)
$La_{0.8}Sr_{0.2}MnO_3$	5.504	13.41	351.8	33.5
$La_{0.75}Sr_{0.25}Cr_{0.9}Ni_{0.1}O_3$	4.477	13.39	347.8	17.9
$La_{0.75}Sr_{0.25}Cr_{0.9}Co_{0.1}O_3$	5.495	13.35	340.0	46.5
$La_{0.75}Sr_{0.25}Cr_{0.9}Fe_{0.1}O_3$	5.498	13.47	352.7	36.6
$La_{0.75}Sr_{0.25}Cr_{0.9}Mn_{0.1}O_3$	5.481	13.38	348.1	20.2

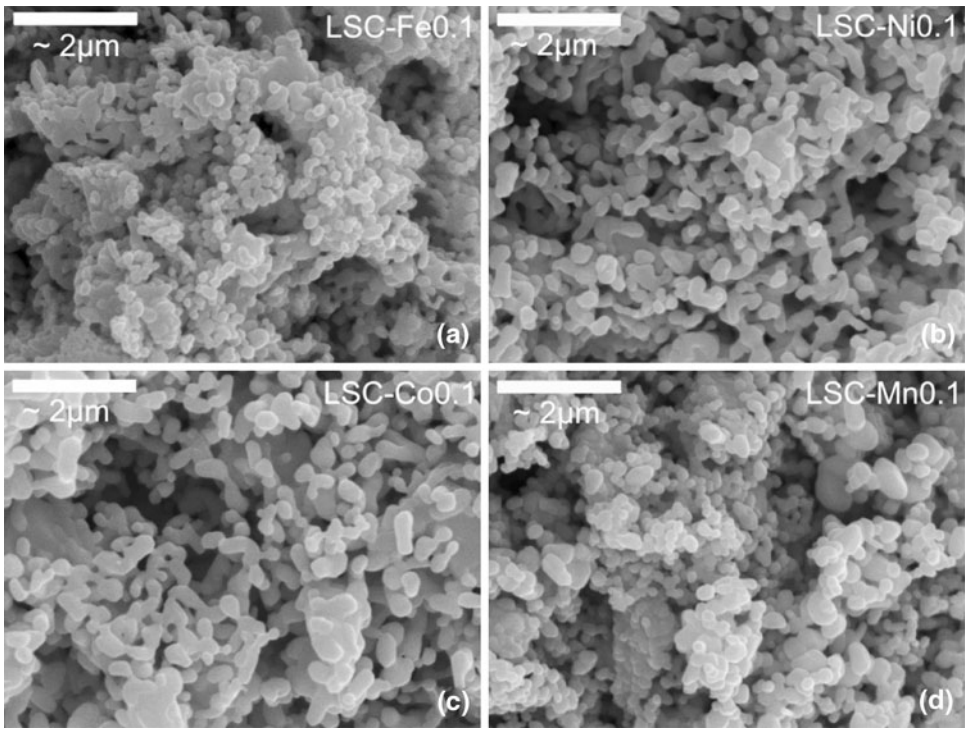

Fig. 2 Scanning electron micrographs of the surface of the LSC-M0.1 electrodes. **a** LSC-Fe0.1, **b** LSC-Ni0.1, **c** LSC-Co0.1 and **d** LSC-Mn0.1

Characteristic cross section SEM images of the anode electrode/electrolyte interfaces for the electrodes LSC-Fe0.1 and LSC-Co0.1 are illustrated in Fig. 3. The average electrode thickness was about 20 μm, in agreement with the measured electrode weight. SEM pictures, both top-view and cross-section, were also taken after the fuel cell testing. The surface morphology and microstructure remained unaffected by the testing conditions. The electrode still had its porous, homogeneous microstructure with adequate adherence to the YSZ electrolyte indicating good thermal compatibility between both materials. No reaction or diffusion region was observed in the electrode/electrolyte interface.

3.2 Performance of button cell SOFCs

The anode materials performance was evaluated using electrolyte-supported cells operating under dry CO/CO_2 mixture (0.9%/0.1% in He balance) vs oxygen (1.36% in He balance). The comparison among the four perovskite anode electrodes at 900 and 1000 °C is presented in Fig. 4, with typical current–voltage and the corresponding power density curves. The theoretical (reversible) open circuit voltage (OCV) under these conditions is 0.944 and 0.900 V for 900 and 1000 °C, respectively. The experimentally observed OCV values deviate by about 30–40 mV from the theoretical ones mainly due to some gas leakage occurring between anode and cathode side of the cell, rather than electronic leakage current through the electrolyte, since YSZ is a pure ionic conductor. In both temperatures, the performance of the perovskite materials in terms of maximum power density follows the sequence Fe > Ni > Co > Mn, based on the B-site substitution cation. The maximum current density measured for the best performing material, the LSC-Fe0.1 perovskite, was 14 and 24 mA cm^{-2} at 900 and 1000 °C respectively, while peak power densities of 2.6 and 4 mW cm^{-2} were obtained at 900 and 1000 °C respectively. As expected, the overall

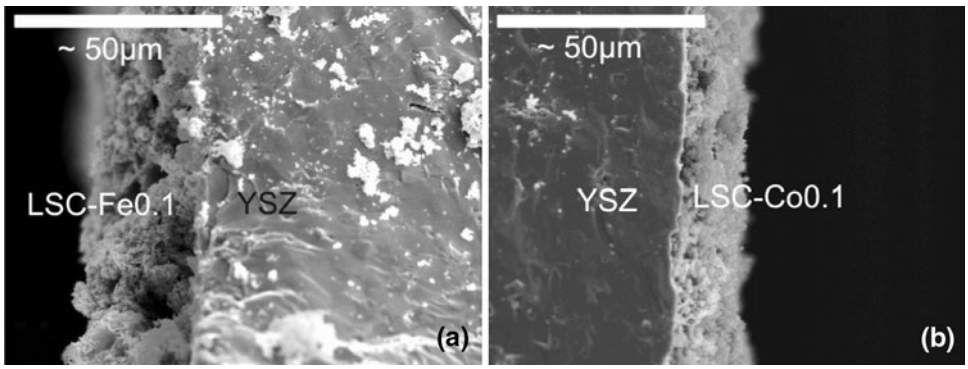

Fig. 3 Scanning electron micrographs of cross-sections of the **a** LSC-Fe0.1 and **b** LSC-Co0.1 electrodes

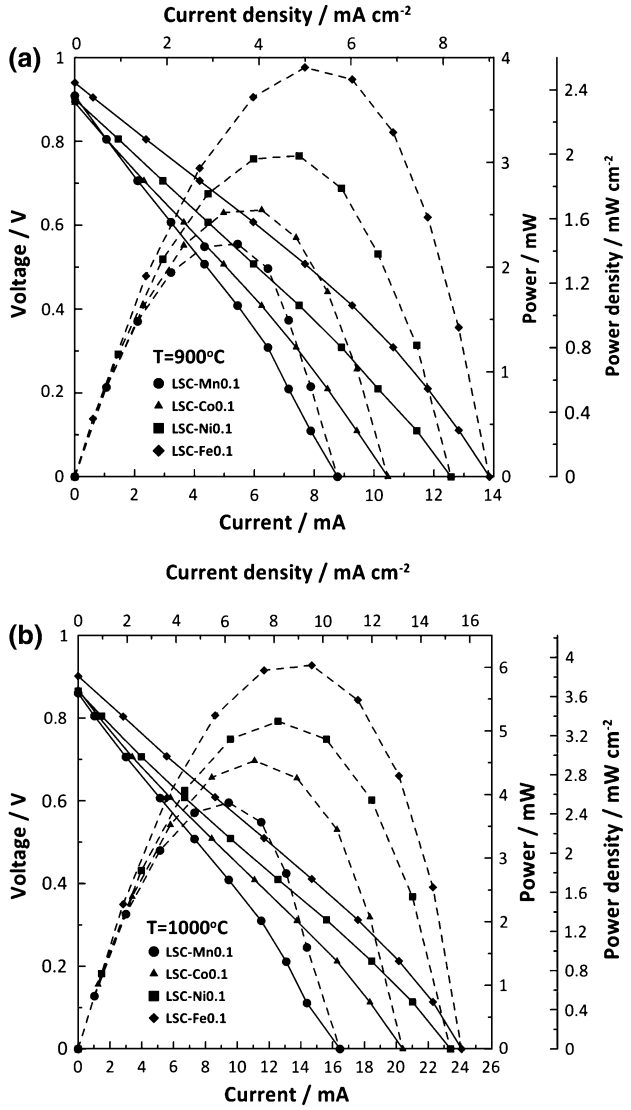

Fig. 4 Fuel cell performance of the LSC-M0.1/YSZ/LSM cell at **a** 900 °C and **b** 1000 °C (CO/CO_2: 0.9%/0.1%; O_2: 1.36% diluted in He)

performance of the fuel cell was enhanced by increasing the operating temperature. The catalytic activity of perovskite oxides has been shown to be highest when the oxide-ion conductivity is high [20]. Doping the B-site of the strontium-doped lanthanum chromites with transition metals creates oxygen vacancies and therefore enhances their CO electrocatalytic activity. The beneficial effect of transition metal substitution on the B site over the base perovskite material (ABO3) has been shown for methane reforming [9] and oxidation [21] as well as for CO oxidation [22]. In the latter case, Fe-based perovskites were the most active catalysts and their activity was increasing with increasing Co/Fe ratio. The superior effect of Fe, among other substitution cations in the perovskite structure, has recently been reported by Danilovic et al for a solid oxide fuel cell utilizing methane as fuel [23].

The area-specific resistances (ASR) have also been calculated for all samples from the slopes of I–V curves at the linear region. They were found to be 0.089 Ω cm^2 for LSC-Fe0.1, 0.103 Ω cm^2 for LSC-Ni0.1, 0.122 Ω cm^2 for LSC-Co0.1 and 0.142 Ω cm^2 for LSC-Mn0.1 at 900 °C. The corresponding ASRs at 1000 °C were 0.0527, 0.0566, 0.0624 and 0.0748 Ω cm^2, respectively. The low power densities obtained are the result of a not fully optimized cell structure in terms of electrolyte thickness, anode and cathode microstructures, which would decrease the electrode polarization. It should also be noted that at the region of high currents (voltage < 0.4 V) a bending on the I–V slopes and a corresponding onset of a limiting current behavior is observed. This may be attributed to fuel starvation since the CO concentration is very low (0.9%) even though the currents are in the range of few mA. Additionally, as reported by Primdahl and Mogensen [24], in some fuel cell anode tests a gas diffusion impedance, related to the stagnant gas outside the porous anode structure but not to the porous anode structure itself, was observed. However, the supposed fuel starvation starts at the voltage range which is well below the applicable limit for fuel cell applications.

It is known that perovskites, especially Fe and Co based ones, tend to react with the zirconia based electrolyte forming the non-conducting $La_2Zr_2O_7$ phase, after prolonged exposure in high operating temperatures [25].

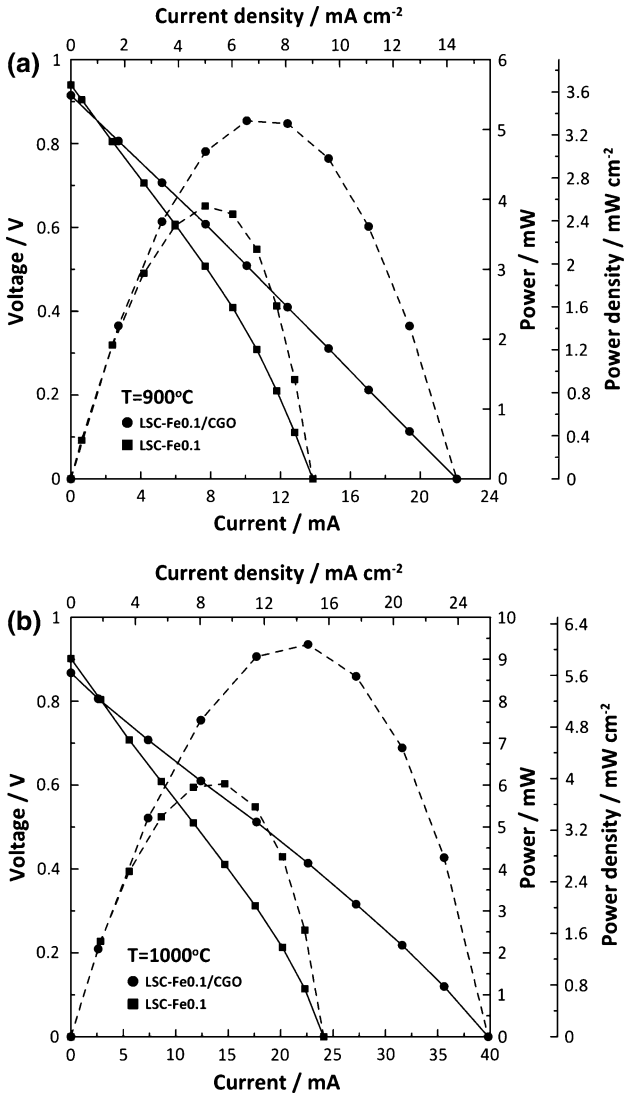

Fig. 5 Fuel cell performance of the LSC-Fe0.1/YSZ/LSM cell at **a** 900 °C and **b** 1000 °C with and without the CGO barrier layer (CO/CO_2: 0.9%/0.1%; O_2: 1.36% diluted in He)

A barrier layer of cerium-gadolinium oxide (CGO) between the perovskite and the electrolyte is commonly used to prevent this reaction and the concomitant degradation of the cell. Therefore, a CGO precursor solution (Gadolinium Doped Ceria, $(Ce_{0.8}Gd_{0.2})O_{1.9}$, GDC20 from NexTech Materials) was applied directly via spraying on the electrolyte followed by firing at 1300 °C, resulting in a thin dense layer of about 20 μm. A LSC-Fe0.1 perovskite film was deposited on top of this film using the standard method described above. The performance of the cell with and without the CGO barrier layer at 900 and 1000 °C is presented in Fig. 5. The addition of CGO layer increases remarkably the performance of the perovskite anode electrodes (the ASRs have been decreased to 0.0622 and 0.320 Ω cm^2 at 900 and 1000 °C, that is by 30–40% as compared to the cell without the CGO layer), although the contrary was observed when used in the cathode side [25]. The latter was attributed to bad adhesion of the CGO layer to the YSZ electrolyte. On the other hand, combined LSCM and CGO anodes are considered as promising materials for fuel cells operating under methane or hydrogen fuels [7]. The beneficial effect of the CGO layer in anode operation maybe related to the porous structure of CGO layer (as compared with dense YSZ support) and the formation of a composite material, perovskite-CGO, with increased electronic conductivity (as the result of the Ce^{+4} to Ce^{3+} reduction) and expanded triple phase boundary area.

A major concern when carbon based fuels are used in SOFC is the formation of carbon which leads to deterioration of electrode performance. In order to detect and reveal carbon deposition on the anode electrodes during fuel cell testing, a temperature programmed oxidation (TPO) cycle was performed after the completion of each fuel cell run. These experiments showed no carbon deposition for the short-range exposure to CO/CO_2 reaction mixtures. However, these TPO experiments represented a single redox cycling of the anode electrodes under high temperatures (900–1000 °C) to which all perovskite materials examined exhibited considerable tolerance and stability. The stability of the LSC-Fe0.1 anode material was furthermore evaluated through a long-term testing, under dry CO/CO_2 composition (1.8%/0.2% in He balance), which lasted for 5 days (120 h). The cell (with the CGO layer) was kept under constant (nominal) potential of 0.65 V and the current output was recorded over time (Fig. 6). A slight decrease of the current produced under this potential is observed. The appearance of wide peaks (4 peaks in the course of current testing) is worth noting, indicating a periodic activation process. In any case, the rate of performance decay seems unaffected from these peaks. The current decrease was of the order of 5.7% through the whole period of 120 h testing. During the first

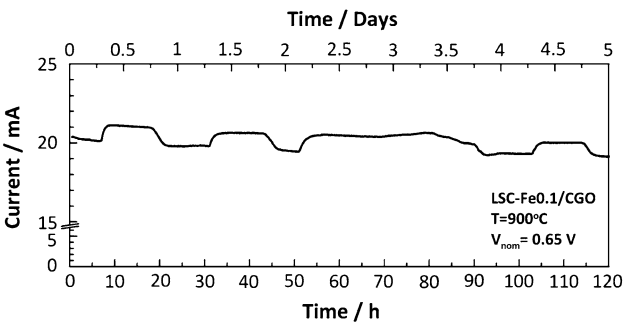

Fig. 6 Long term testing of the cell LSC-Fe0.1/CGO//YSZ//LSM-YSZ/LSM. (CO/CO_2: 1.8%/0.2%; O_2: 2.53% diluted in He; $T = 900$ °C; $V_{nom} = 0.65$ V)

50 h of operation the decrease was about 4.5% while only 1.2% corresponds to the rest 70 h. This behavior is indicative for the absence of massive carbon deposition and this was further supported by the fact that no CO_2 signal was detected during temperature programmed oxidation (TPO) run after the long term exposure to CO.

It should be emphasized that the purpose of present work at this stage was to validate the preparation method and evaluate comparatively the performance of the different perovskite materials as anodes for CO-fueled SOFCs. Having identified the most promising material, specifically LSC-Fe0.1, the minimization of ohmic resistances and the corresponding apparent ASR is expected by the use of thin (of the order of few μm) electrolyte layers. Preliminary experiments utilizing electrochemical impedance spectroscopy (EIS) indicate that the major part of the apparent overall ASR is due to electrolyte resistance.

4 Conclusions

A series of $La_{0.75}Sr_{0.25}Cr_{0.9}M_{0.1}O_3$ (M = Mn, Fe, Co, Ni) perovskite compositions were prepared by the modified citrate/sol gel route. The prepared powder materials were tested as anodes for CO-fueled SOFCs in the form of LSCM/YSZ/LSM cells. The steady state performance in the $CO/CO_2:O_2$ system revealed the superior performance of the LSC-Fe0.1 composition for the temperature range of 900–1000 °C. Further research is under way in order to define the resistance components and optimize the cell performance by the use of thin electrolyte films.

Acknowledgments The authors are thankful to the European Space Agency (ESA) for funding this work under Contract No. 21767/08/NL/LvH. Thanks are also due to O. Orfanou, T. Vavaleskou and G. Traskas for performing the XRD, ICP and SEM measurements.

References

1. Hawkes A, Leach M (2005) J Power Sources 149:72
2. Sauvet AL, Fouletier J (2001) Electrochim Acta 47:987
3. Caillot T, Gélin P, Dailly J, Gauthier G, Cayron C, Laurencin J (2007) Catal Today 128:264
4. Bebelis S, Neophytides S, Kotsionopoulos N, Triantafyllopoulos N, Colomer MT, Jurado J (2006) Solid State Ionics 177:2087
5. Park SD, Vohs JM, Gorte RJ (2000) Nature 404:265
6. Gorte RJ, Kim H, Vohs JM (2002) J Power Sources 106:10
7. Tao S, Irvine JTS (2004) J Electrochem Soc 151:A252
8. Liu J, Madsen BD, Ji ZQ, Barnett SA (2002) Electrochem Solid State 5:A122
9. Sfeir J, Buffat PA, Möchli P, Xanthopoulos N, Vasquez R, Mathieu HJ, van Herle J, Ravindranathan Thampi K (2001) J Catal 202:229
10. Ruiz-Morales JC, Canales-Vázquez J, Ballesteros-Pérez B, Peña-Martínez J, Marrero-López D, Irvine JTS, Núñez P (2007) J Eur Ceram Soc 27:4223
11. Atkinson A, Barnett S, Gorte RJ, Irvine JTS, McEvoy AJ, Mogensen M, Singhal SC, Vohs J (2004) Nat Mater 3:17
12. Tao S, Irvine JTS (2004) Chem Rec 4:83
13. McIntosh S, Gorte RJ (2004) Chem Rev 104:4845
14. Pipoli T, Besenhard JO, Schautz M (2002) In situ production of fuel and oxidant for a small solid oxide fuel cell on Mars. In: Wilson A (ed) Sixth European Space Power Conference (ESPC). ESA Publications Division (Noordwijk), Porto, Portugal
15. Sfeir J, Herle Jv, McEvoy AJ (1999) J Eur Ceram Soc 19:897
16. Kong J, Zhang Y, Deng C, Xu J (2009) J Power Sources 186:485
17. Konysheva E, Irvine JTS, Besmehn A (2009) Solid State Ionics 180:778
18. Zha S, Tsang P, Cheng Z, Liu M (2005) J Solid State Chem 178:1844
19. Rousseau S, Loridant S, Delichere P, Boreave A, Deloume JP, Vernoux P (2009) Appl Catal B-Environ 88:438
20. Fergus JW (2006) Solid State Ionics 177:1529
21. Tan X, Li K, Thursfield A, Metcalfe IS (2008) Catal Today 131:292
22. Kournoutis V (2010) PhD Thesis, University of Patras
23. Danilovic N, Vincent A, Luo J-L, Chuang KT, Hui R, Sanger AR (2010) Chem Mater 22:957
24. Primdahl S, Mogensen M (1999) J Electrochem Soc 146:2827
25. Kammer Hansen K, Menon M, Knudsen J, Bonanos N, Mogensen M (2010) J Electrochem Soc 157:B309